

pubs.acs.org/joc Article

Late-Stage Modification of Electronic Properties of Antiaromatic and Diradicaloid Indeno[1,2-b]fluorene Analogues via Sulfur Oxidation

Justin J. Dressler, Joshua E. Barker, Lucas J. Karas, Hannah E. Hashimoto, Ryohei Kishi, Lev N. Zakharov, Samantha N. MacMillan, Carlos J. Gomez-Garcia, Masayoshi Nakano, Judy I. Wu, and Michael M. Haley*



Cite This: J. Org. Chem. 2020, 85, 10846-10857



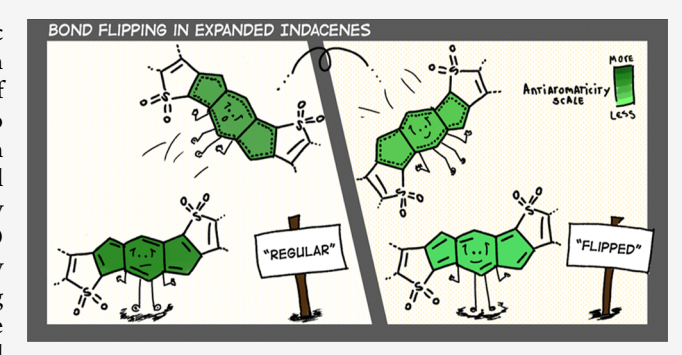
ACCESS

Metrics & More



s) Supporting Information

ABSTRACT: The ability to alter optoelectronic and magnetic properties of molecules at a late stage in their preparation is in general a nontrivial feat. Here, we report the late-stage oxidation of benzothiophene-fused indacenes and dicyclopentanaphthalenes to their corresponding sulfone derivatives. We find that while such modifications increase the highest occupied molecular orbital (HOMO)—lowest unoccupied molecular orbital (LUMO) energy gap to a small degree, other properties such as HOMO and LUMO energy levels, molecule paratropicity, and singlet-triplet energy gaps are influenced to a greater degree. The most surprising finding is a change of the bond alternation pattern within the s-indacene core of the sulfones. Computations corroborate the experimental



findings and offer plausible explanations for these changes in molecular properties.

■ INTRODUCTION

Recently, there has been resurgent interest in polycyclic conjugated hydrocarbons (PCHs) that possess unique properties for application in organic electronics. The earliest and most promising PCH targets were acenes; 1-4 however, these compounds are prone to oxidative degradation. 3,5,6 In an attempt to develop suitable acene alternatives with decreased aromaticity that retain the π -conjugation integral to the high charge carrier mobility of acenes, PCHs that possess antiaromatic character have become fruitful avenues of research. Defined as cyclic, planar, fully conjugated systems with (4n) π -electrons,⁸ antiaromatic molecules often display properties such as decreased delocalization, narrow highest occupied molecular orbital (HOMO)—lowest unoccupied molecular orbital (LUMO) energy gaps, 9-11 paratropic proton nuclear magnetic resonance (NMR) chemical shifts, and concomitant large positive nucleus-independent chemical shift (NICS) values. 12,13 A common strategy to generate antiaromatic hydrocarbons that are closely related to acenes is to replace one or more six-membered rings with either a fouror five-membered carbonaceous ring.7 This approach over the past decade has resulted in a wide range of antiaromatic compounds based mainly on pentalenes, 14-22 cyclobuta-dienes, 23-26 and indacenes, 27-33 among others. The research on such molecules was in part fueled by the Breslow group's hypothesis that reduced aromaticity/increased antiaromaticity has the potential to increase molecular conductivity. 34-37 Very recent studies support this notion as organic field effect

transistors (OFETs) with antiaromatic molecules as the semiconducting layer can now exhibit average hole-mobilities that are >1 cm 2 V $^{-1}$ s $^{-1}$. 23,25,38,39

Another group of PCHs accruing interest are those that display diradical character. The recent increase in reports of carbon-based diradicaloids has also been driven by their potential applications both in organic electronics 40,41 and as magnetic materials. 42-45 The desire to gain a better fundamental understanding of these compounds, which possess a unique set of properties (e.g., narrow HOMO-LUMO gaps, 40 low-lying doubly excited electronic energy absorptions, 46,47 and electronic spin resonance signals 48), has led to synthesis of various families of diradicaloids based on bisphenalenyls, 41,49-51 zethrenes, 52-55 indenofluorenes, 56,57 and closely related diindenoacenes, 58-65 among others. Through the study of these different classes of diradicals, a common theme has been unearthed, that the two concepts of antiaromaticity and diradical character are interrelated. In many cases, antiaromatic molecules, once π -expanded, reveal a tendency to assume an aromatic, open-shell resonance

Received: June 11, 2020 Published: July 17, 2020





Figure 1. New IDBTs 1 and 2, known IIDBTs 3 and 4, their sulfone analogues 5-8, and the decomposition product 9.

structure in the ground state to relieve the antiaromaticity of the conjugated, closed shell core.⁶⁶

Utilizing the indeno [1,2-b] fluorene framework, our group in recent years has aspired to tune both antiaromaticity (in benzene core molecules) and diradical character (naphthalene and larger aromatic cores) through two different approaches, either by changing the fusion bond order on both sides of the s-indacene core^{28,63} or by adding benzothiophene units in the same position (anti or syn to the apical carbon in the fivemembered ring, e.g., 1-4 in Figure 1) to modulate electronic properties. 27,60,62,67 These studies have provided key insights into what electronic factors can be altered to tune either the antiaromaticity (i.e., fusion bond order)227,28 and/or the diradical character (i.e., electronic repulsion factor and the transfer integral term)60,62 in a series of structurally related molecules.⁶⁸ Such approaches have relied heavily on early synthetic modification to impart changes in the chemical connectivity to drive a concomitant change in properties. These modifications are manifested either by π -extending the acene core, requiring a change to the synthetic route very early on or through altering the outer fused rings that required synthetic changes during the key carbon-carbon bondforming steps; nonetheless, the amount of synthetic work needed to tune these properties was demanding, often requiring entirely new preparative routes.

Our recent studies on indacenodibenzothiophenes^{27,67} (IDBTs, e.g., 1, 2) and indenoindenodibenzothiophenes^{60,62} (IIDBTs, e.g., 3, 4) provide a unique opportunity for late-stage modification of the electronics of our molecules, from electronrich to electron-poor, through the conversion of the sulfur atoms to fully oxidized sulfones (e.g., IDBT-S 5–6 and IIDBT-S 7–8). A relevant report from the Campos group,⁶⁹ among others,^{70–73} has shown that oxidation of sulfur in polythiophene lowers the LUMO energy level and thus affords an overall change in the properties of the bulk material. Herein, we report the synthesis and detailed characterization of sulfones 5, 6, and 8 and computationally corroborate that changing the oxidation state of the sulfur has profound effects

on the antiaromaticity and diradical character of the molecules. This work looks to highlight the ability to impart overall large-scale electronic modification to the molecules, tuning the targeted properties, utilizing a nonarduous synthetic route.

■ RESULTS AND DISCUSSION

Synthesis. Our initial efforts started with the known mesityl (2,4,6-trimethylphenyl) analogues of 1 and 2.²⁷ While we successfully oxidized the former to 5-Mes (see the Experimental Section for details), oxidation of the latter afforded an insoluble and uncharacterizable violet solid. We then switched to 2,6-dimethyl-4-t-butylphenyl units (which we have coined t-Mes) on the apical carbons as these confer considerably improved solubility. Reacting 2,6-dimethyl-4-tbutylphenyllithium with diones 10 and 11 (Scheme 1) followed by an acidic aqueous workup gave intermediate diols (not shown) that were reductively dearomatized using SnCl₂ and catalytic trifluoroacetic acid (TFA) to furnish the fully conjugated IDBTs 1 and 2, respectively. IIDBTs 3 and 4 were prepared analogously from diones 12 and 13 as previously reported. 60,82 Oxidation of the fully conjugated scaffolds utilizing meta-chloroperoxybenzoic acid (mCPBA) successfully resulted in purple sulfones 5, 6, and 8 in modest to moderate yields. Surprisingly, oxidation of anti-IIDBT 3 with mCPBA did not furnish sulfone 7 but rather an uncharacterizable orange solid whose absorption spectrum lacked the characteristic low energy bands >500 nm (Figure S8), suggestive of a system with less than expected π -conjugation. We explored other oxidizing reagents such as H₂O₂, oxone, and urea-hydrogen peroxide (UHP). Only the reaction of 3 with UHP proceeded to afford a purple solid in low yield, which we initially believed to be the desired sulfone as the compound possessed low energy transitions out to ~640 nm (Figure S9) and an appropriate ¹H NMR spectrum (see Supporting Information); however, the structure obtained by X-ray diffraction (XRD) (vide infra) revealed it to be molecule 9 as shown in Figure 1. This structure suggests that compound 7 likely was formed during the reaction but the oxidized ring

Scheme 1. Synthesis of IDBTs 1, 2, and IIDBT 3, 4 and Their Conversion to the Respective Sulfones 5–8 along with Formation of Decomposition Product 9

hydrolyzed/cleaved (ArSO₂— is a reasonable leaving group), urea next condensed onto the newly formed ketone carbonyls, and then the system recyclized in some manner to afford 9. Regardless of how 9 is generated, we never observed direct evidence of 7. Out of chemical curiosity, less π -conjugated anti-IDBT 1 was subjected to oxidation conditions using UHP, which furnished only a trace amount of an analogous sulfonamide (as only detected by mass spectrometry). This outcome suggests that the anti-orientation of the proaromatic core of 7 is prone to degradation to regain naphthalene aromaticity as found in 9, something we have not observed in any of our prior IIDBT studies.

NMR Spectroscopy and NICS-XY Scans. Because the central protons on the IDBTs are directly attached to the sindacene core, one would expect these protons to be sensitive to the paratropic environment and experience an upfield chemical shift. Indeed, this is the case: whereas the ¹H NMR chemical shift of the central six-membered ring protons of the parent indeno[1,2-b]fluorene is 6.85 ppm, these analogous protons in the previously reported Mes-substituted anti-IDBT and syn-IDBT appear at 6.11 and 6.06 ppm, respectively, in line with the claim of increased antiaromaticity of the sindacene core of the IDBTs.²⁷ In the current study, substitution with t-Mes affords values of 6.09 and 6.06 ppm for 1 and 2, respectively (Figure 2a). In both cases, the syn derivative is slightly more upfield than the anti isomer, indicating the syn is slightly more paratropic, a result corroborated by NICS-XY scan calculations (vide infra).²⁷ Intriguingly, after sulfone formation, this trend is reversed, the core singlet for syn-IDBT-S 6 appears at 6.91 ppm and for anti-IDBT-S 5 at 6.03 ppm, the latter result suggesting that the paratropic core of 5 is comparable to that of 1 and 2.

Given the difficulty of assessing aromaticity/antiaromaticity based solely on relatively small changes of NMR chemical shifts, we computationally explored the ring currents of IDBT-

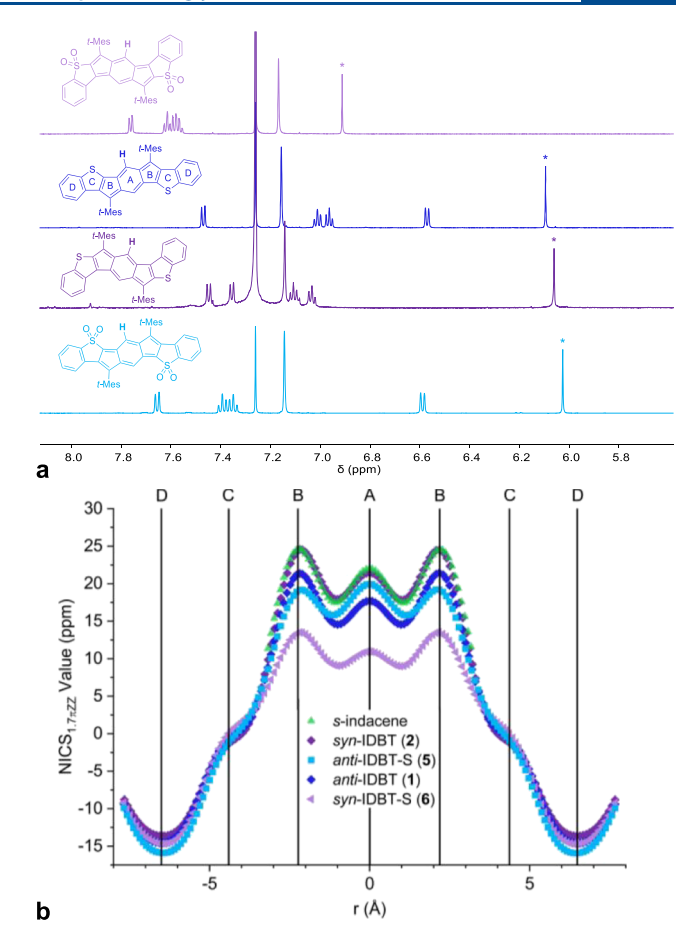


Figure 2. (a) Proton NMR spectra of the aromatic region of IDBTs 1 and 2 and the corresponding sulfones 5 and 6. The central proton (*) displayed in bold in the structures on the left can be used to roughly assess antiaromaticity. (b) NICS-XY scans for IDBTs 1 and 2 and sulfones 5 and 6 along with the scan for the parent s-indacene, in order of most to least paratropic; for clarity, the ring labels are shown above in the structure of 5.

S 5 and 6 using NICS-XY scans, as these allow us to explore areas of the molecule that possess both paratropic and diatropic ring currents within the same system. 74,75 All calculations were performed with the unsubstituted structures to decrease computational cost as exclusion of the mesityl groups has been shown to have a negligible impact on the NICS-XY results.²⁸ Notably, all the IDBT derivatives possess a paratropic s-indacene-like core (Figure 2, rings A and B). The NICS scans (Figure 2b) replicate our prior studies that showed that the syn-IDBT core of 2 is nearly as antiaromatic (21-24 ppm, dark-purple) as s-indacene itself (22-25 ppm, green), whereas the anti-IDBT core of 1 is slightly less paratropic (18-21 ppm, dark-blue). In all cases, the thiophene rings (C) appear to be atropic (0 to -1 ppm), regardless of the sulfur oxidation state, and similarly all the outer benzene rings (D) possess strong aromaticity with minimal variation (-14 to -16ppm). Interestingly, oxidation reverses the syn/anti ordering, where syn-IDBT-S 6 has weaker paratropicity (11-13 ppm, light-purple) compared to IDBTs 1 and 2, and anti-IDBT-S 5 shows comparable paratropicity (19–20 ppm, light-blue) to 1. In fact, the NICS values for ring A are essentially the same for 2 and 5, which support their near-identical chemical shifts in the aforementioned proton NMR experiments.

Figure 3. Selected resonance forms for the hydrocarbon dianion reference analogues of (a) syn-IDBT 2 and (b) anti-IDBT 1; boxed structures are the dominant resonance forms recognized by NBO.

Further calculations suggest there are two competing effects that influence the antiaromatic characters of the parent IDBTs (1 vs 2) and the corresponding sulfones (5 vs 6)—a "Clar sextet-effect" and a "charge-effect", respectively. When a Clar sextet-effect dominates, the compound with more quinoidal character will have a smaller HOMO–LUMO energy gap (e.g., syn-IDBT 2). When a charge-effect dominates, the less charge-stabilized compound will have a smaller HOMO–LUMO gap (e.g., anti-IDBT-S 5). A smaller HOMO–LUMO gap often translates to greater antiaromatic character because the HOMO–LUMO gap is a denominator in the paramagnetic term of the equation used to compute magnetic shielding. Whether a Clar sextet-effect or charge-effect dominates depends on the electronegativity of the heteroatom(s).

Calculations suggest that the stronger paratropicity of 2 (dark-purple curve, Figure 2b) versus 1 (dark-blue) is the result of a less aromatic resonance structure (i.e., a "Clar sexteteffect"). Computed natural bond orbital (NBO) analyses for the isoelectronic hydrocarbon "dianion" reference analogues of the benzothiophene-fused s-indacenes (i.e., syn- and anti-IDBT) show that the dominant resonance form of the syn-IDBT reference is a quinoidal resonance structure (boxed structure in Figures 3a and S24 for the NBO output), while that of the anti-reference displays two Clar sextets in the terminal benzenoid rings (boxed structure in Figures 3b and S25 for the NBO output).⁷⁶ In concert, the computed $NICS(1.7)_{\pi zz}$ values show a less negative value for 2 (-14) ppm) and a more negative value for 1 (-15 ppm) at the terminal benzene rings (ring D in Figure 2b). The more paratropic syn-IDBT also has a smaller computed HOMO-LUMO gap (1.84 eV) compared to that of anti-IDBT (1.96 eV).

As shown experimentally, IDBT-S $\mathbf{5}$ and $\mathbf{6}$ display the opposite trend, that is, a "charge-effect" dominates. Sulfone $\mathbf{5}$ (light-blue trace in Figure 2b) is significantly more paratropic than $\mathbf{6}$ (light-purple) because the electronegative sulfone (SO₂) groups are placed at topologically disfavored positions, resulting in a narrower HOMO–LUMO gap and increased antiaromatic character. As shown in Figure 4, computed

Figure 4. NPA charges for s-indacene.

natural population analyses (NPA) charges for s-indacene are the most negative at carbons 2 and 6. Because of this charge distribution, fused ring arrangements that stabilize negative charges at carbons 2 and 6 will stabilize the s-indacene core. When SO₂ groups are fused to s-indacene in a syn arrangement, the electronegative SO₂ groups are placed at positions that help stabilize negative charges at carbons 2 and 6. For this reason, 6 exhibits a larger HOMO-LUMO gap (1.95 eV, Table S1) and decreased paratropicity. When SO₂ groups are fused to s-indacene in an anti arrangement, the SO₂ groups are connected to carbons 3 and 7 (the least negatively charged positions), and this stabilizes the s-indacene core to a lesser extent. As a result, anti-IDBT-S 5 exhibits a narrower HOMO-LUMO gap (1.65 eV), that is, increased paratropicity. The charge effect described here is akin to the rule of topological charge stabilization, first proposed by Gimarc to explain how the placement of heteroatoms in hydrocarbon frameworks affect the relative stabilities of the possible isomers.7

It is worth noting that even though both Clar sextet effects and charge effects are present in the parent and sulfone compounds, differences in the antiaromatic characters of *syn* versus *anti*-IDBT are dominated by the Clar sextet effect, while the *syn*-versus *anti*-sulfones set is influenced more so by the charge effect because of the stronger electronegativity of the sulfones. To further illustrate the competing Clar sextet and charge effects, the NICS-XY scans of *syn*- and *anti*-IDT and *syn*- and *anti*-IDT-S were performed at the same level of theory (Figures S21 and S22). The scans showed that without the terminal benzene rings (no Clar sextet-effect), both the IDT and IDT-S compounds show a more paratropic *anti*-form because of a dominating charge effect. It is also worth noting the more pronounced difference in paratropicity for the IDT-S pair (Figure S22).

Electronic Absorption Spectroscopy. Sulfones 5, 6, and 8 exhibit UV–vis–near-infrared absorption spectra (Figure 5) very similar to their respective thiophene parents (1, 2, and 4). All of the molecules possess strong absorptions in the range of 300–400 nm. Interestingly, the main difference between the thiophene and sulfone compounds is displayed in the lowenergy absorptions, where all of the sulfones show a blue-shift of the main low energy absorption anywhere from 8 nm in compound 6 to as large as 37 nm in 5. While the π -extended nature of the IIDBTs red-shifts the low-energy absorption appreciably (~100 nm), IIDBT-S 8 also is blue-shifted 24 nm

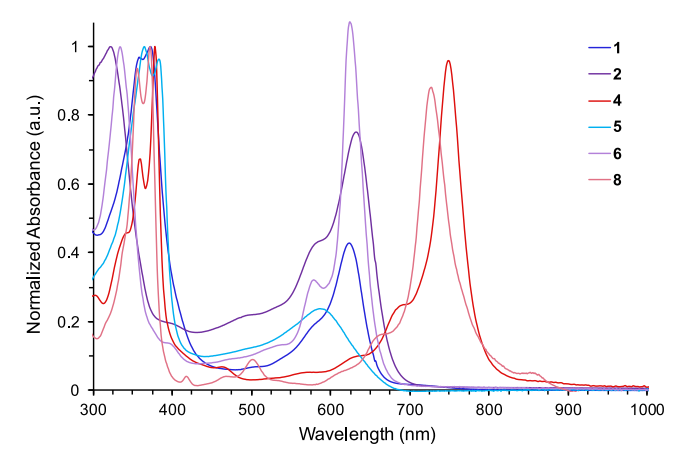


Figure 5. Electronic absorption spectra of the three stable sulfones **5**, **6**, and **8** and their parent thiophenes **1**, **2**, and **4** in CHCl₃ at room temperature. The spectrum of each sulfone is of a color similar to the parent compound, with the sulfone having the lighter hue.

compared to parent 4, suggesting all three sulfones possess slightly larger optical energy gaps. Gratifyingly, the time-dependent density functional theory-generated absorption spectra (Figures S4–S7) corroborate these changes for all sulfones; specifically, the calculations replicate that *anti-5* would display a greater blue-shift in the low-energy absorption than *syn-6*, a trend also predicted for the naphthalene series (*anti-7* vs *syn-8*) as well. Another interesting feature observed for compounds 4 and 8 is a weak absorption shoulder (852 and 866 nm, respectively) in the low-energy absorption due to a low-lying doubly excited electronic configuration, a common occurrence in molecules with appreciable open-shell character (vide infra). 46,47

Electrochemistry. To further probe their electronic properties, cyclic voltammetry of sulfones 5/6/8 was carried out in CH_2Cl_2 (Figure 6). The redox behavior of the sulfones

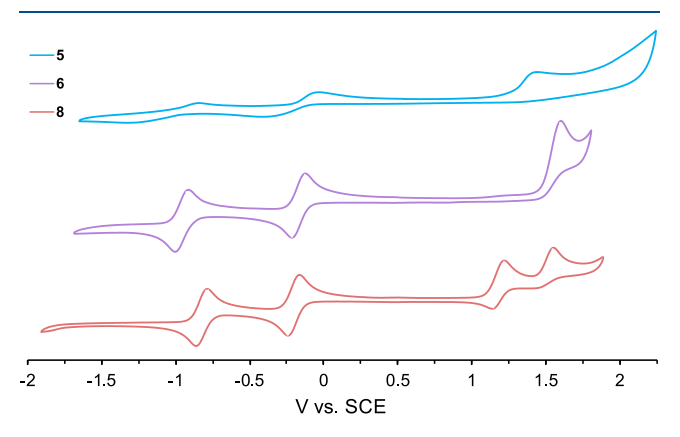


Figure 6. Cyclic voltammograms of 5, 6, and 8.

compared to their thiophene precursors are shown in Figures S10–S12, with the results compiled in Table 1. All of the sulfones undergo a reversible first reduction in solution along with a second reduction that is reversible for 6 and 8 and pseudoreversible for 5. IDBT-S 5 and 6 exhibit one irreversible oxidation, while IIDBT-S 8 displays one reversible oxidation followed by a second irreversible oxidation. $E_{\rm red1}$ values range from -0.17 to -0.22 V versus the saturated calomel electrode (SCE) and $E_{\rm ox1}$ values range from 1.18 to 1.60 V versus SCE. In our prior studies, comparison of the electrochemistry of

parent IDBTs (1 and 2) showed that the syn-IDBT had the narrower HOMO-LUMO energy gap, in agreement with the fact that 2 was more antiaromatic.²⁷ Whereas the HOMO levels of 1 and 2 are comparable, 2 has a lower LUMO leading to the decreased energy gap. In the case of the IDBT-S, the trend is reversed—the LUMOs of 5 and 6 are essentially equal in energy, but it is the higher-in-energy HOMO that leads to the decreased electrochemical energy gap in 5. Given that HOMO-LUMO energy gaps generally narrow with increased antiaromaticity, this supports the finding that once oxidized, 5 is the more antiaromatic of the two. These experimental observations are well-reproduced by quantum chemical calculations (Table S1). Gratifyingly, the electrochemical data for 8 match DFT calculations well, in that the HOMO-LUMO energy gap is calculated to be approximately 1.52 eV, and the experimental value was 1.38 eV. As with the benzene-core sulfones, the HOMO and LUMO energy levels experimentally and computationally are overall lower (more negative) for syn-IIDBT-S 8 when compared to the parent syn-IIDBT 4. A general trend from these studies is that all three sulfones possess overall lower-energy HOMO and LUMO levels (HOMO < -5.8 eV, LUMO < -4.4 eV) relative to the parent thiophenes (HOMO < -5.3 eV, LUMO < -3.8 eV).

Solid-State Structures. To gain insight into the molecular structure of the electronically altered sulfones, single crystal XRD and subsequent bond length analysis of the structures was performed. Slow diffusion of CH₂CN into CHCl₂ solutions of the corresponding compounds gave deep violet crystals of 5-Mes and 9, whereas to attain strongly diffracting crystals for 6 and 8, 3-5 mg of the target compound was dissolved in a 15:1 mixture of CHCl₃ and CH₃CN, which then slowly evaporated over several weeks to obtain suitable crystals for XRD.⁷⁸ The resultant structures and calculated geometries (Figures S27-S30) are shown in Figure 7. Whereas molecules of 5-Mes pack roughly as 1D stacks with a distance of 3.51 Å between the average planes of the central fragments (Figure S14), 6, 8, and 9 pack as isolated molecules with no close $\pi - \pi$ contacts because of the orientation of the bulky t-Mes groups and/or the presence of solvent molecules (Figures S16, S18, and S20). As is typical of benzene- and naphthalene-based quinoidal systems, the molecules show distinct bond alternation about the antiaromatic core. Surprisingly, the bonding pattern in both the IDBT-S and IIDBT-S is flipped as a result of oxidation, as depicted in Figure 8. In fact, out of 50+ X-ray structures of our quinoidal molecules obtained over the past decade,²⁹ the three sulfones are the only molecules to have this flipped arrangement. Nonetheless, all the experimental bond lengths (black numbers in Figure 7) of the hydrocarbon cores are in relatively good agreement with the predicted values (<0.01 Å, blue numbers). All four structures possess bond lengths that suggest the two external sixmembered rings behave as isolated benzenes, in line with the NICS-XY scans. All three sulfone structures display asymmetric carbon-sulfur bond lengths on either side of the S atom where the shorter bond is from the sulfone to the core. Interestingly, the computations overestimate all of the C-S bond lengths by ~0.03 Å. The bond lengths for 9, which are only experimental numbers, are typical of those found in a ring-fused naphthalene.

As depicted in Figure 8a, the bond alternation pattern in all three sulfones changes from the "normal" arrangement (left) to the "flipped" arrangement (right), and the computations corroborate these findings. Plunkett and co-workers discovered

Table 1. Cyclic Voltammetry Data for Thiophenes 1, 2, and 4 and Sulfones 5, 6, and 8^a

cmpd	$E_{\rm red2}$ (V)	$E_{\rm red1}$ (V)	$E_{\rm ox1}$ (V)	$E_{\rm ox2}$ (V)	E_{HOMO} (eV)	E_{LUMO} (eV)	E_{gap} (eV)
anti-IDBT (1)	-1.72	-0.87	0.84	1.32	-5.52	-3.81	1.71
anti-IDBT-S (5)	-1.08	-0.22	1.44		-6.12	-4.46	1.67
syn-IDBT (2)	-1.37	-0.75	0.86	1.57	-5.54	-3.93	1.61
syn-IDBT-S (6)	-0.96	-0.17	1.60		-6.28	-4.51	1.77
syn-IIDBT (4)	-1.23	-0.67	0.66	1.09	-5.34	-4.01	1.33
syn-IIDBT-S (8)	-0.82	-0.20	1.18	1.55	-5.86	-4.48	1.38

"CVs were recorded at a scan rate of 50 mV s⁻¹ with a glassy carbon working electrode, Pt coil counter electrode, and Ag wire pseudoreference. All data were collected in degassed CH_2Cl_2 , and ferrocene was used as an internal reference. Potentials were referenced to the SCE by using the Fc/Fc^+ half-wave potential ($Fc/Fc^+ = 0.46 \text{ C}$ vs SCE).

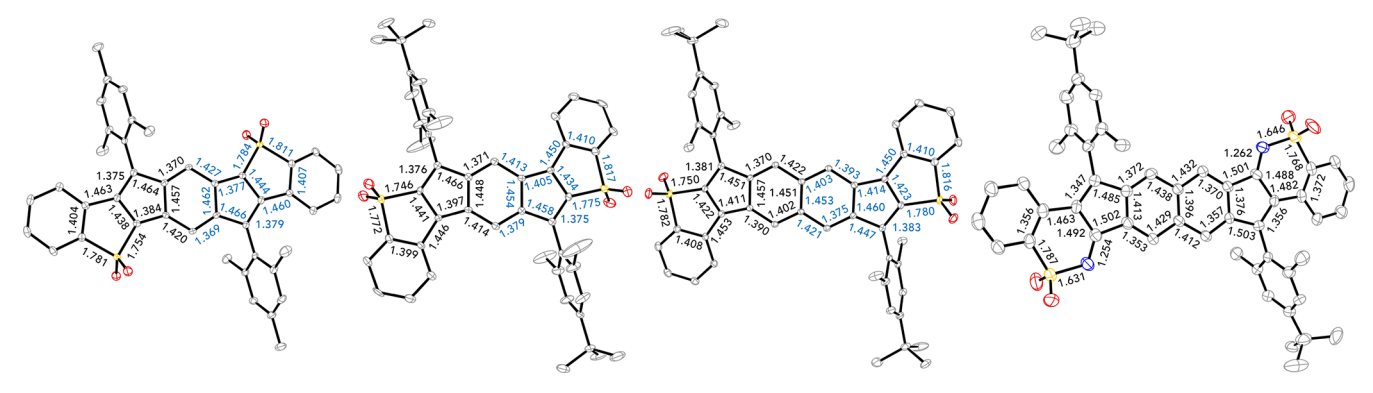


Figure 7. X-ray structures of (left to right) sulfone derivatives 5-Mes, 6, and 8 and decomposition product 9 with selected bond lengths (Å; experimental values in black, calculated values in blue); ellipsoids drawn at the 50% probability level. Experimental numbers for 6 represent the average value from two crystallographically independent molecules.

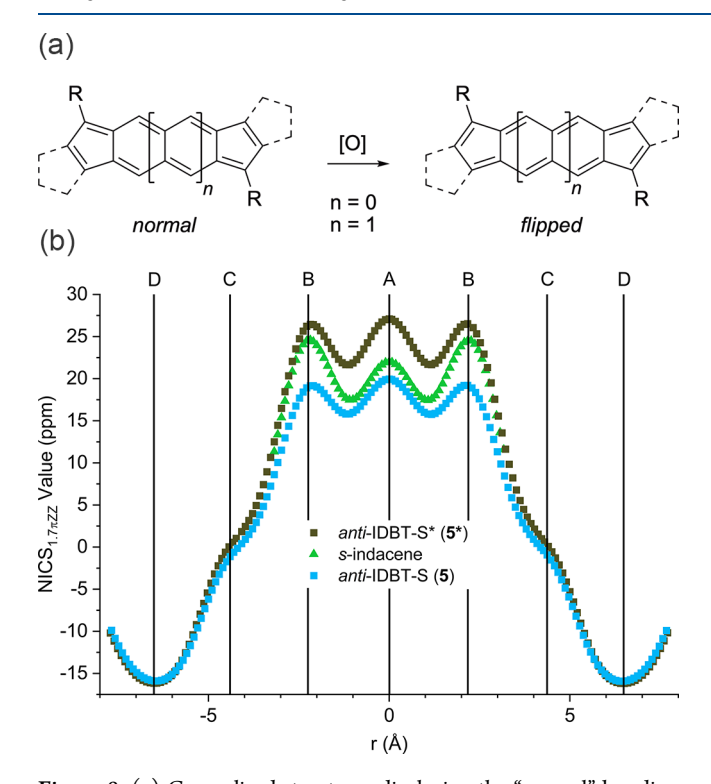


Figure 8. (a) Generalized structures displaying the "normal" bonding pattern observed in most indeno[1,2-*b*]fluorene-based molecules and the "flipped" bonding pattern observed for sulfones **5**, **6**, and **8**. (b) NICS-XY scans of both *anti*-IDBT-S geometries, where **5** is the observed bond-flipped orientation, and **5*** is the normally observed bonding pattern.

a similar bonding pattern reversal for an acenaphthylene-fused pentalene, but their rationale of the molecule adopting the [5] radialene orientation of the double bonds similar to C_{60} and related "buckybowls"²⁰ is clearly not applicable for our molecules. While calculations identified only a bond-flipped structure for 6, two minima structures were found for 5—a higher-energy structure with the normal bond alternation pattern and a flipped structure that was 1.5 kcal mol⁻¹ lower in energy.⁷⁹ NICS-XY scan calculations of 5 and its normal bonding pattern isomer 5* provide a plausible explanation (Figure 8b) for the bond-flipped behavior: whereas the NICS scan of 5 shows reduced paratropicity compared to s-indacene, the NICS scan of 5* suggests that a normal bond alternation arrangement would afford a molecule with greater paratropicity than s-indacene. Because antiaromaticity is a destabilizing feature, the sulfones simply adopt a bond alternation pattern to minimize their paratropicity and thus maximize their overall stability. Computational reevaluation of the Plunkett group's pentalene using NICS-XY scans (Figure S23) reveals that flipping of the bond alternation pattern results in a significant reduction in paratropicity compared to normal pentalene bonding, a result consistent with the above arguments.

Diradical Character of 8. We recently disclosed the synthesis and characterization of IIDBTs 3 and 4, which are rare examples of singlet ground-state diradicaloids that required heating to 100-150 °C in order to access their triplet spin state. The uniquely large singlet-triplet energy gaps (7–8 kcal mol⁻¹) that the IIDBTs display are in part explained by the electronic repulsion of the lone pairs on the sulfur atoms. If we were to remove participation of the sulfur lone pairs by changing them into sulfones as in 7 and 8, we would expect an accompanying change in the singlet-triplet energy gap ($\Delta E_{\rm ST}$) and the diradical character index (y). As

shown in Table S2, the computational results reveal that sulfone formation slightly decreases y (anti -0.012, syn -0.006) and increases $\Delta E_{\rm ST}$, more so for the anti isomers (3 \rightarrow 7, $\Delta \Delta E_{\rm ST} = 0.88$ kcal mol⁻¹) than the syn isomers (4 \rightarrow 8, $\Delta \Delta E_{\rm ST} = 0.23$ kcal mol⁻¹). These results are also in line with the linear (3/7) versus cross conjugation (4/8) arguments of the S atom with respect to the radical center accounting for the differences in IIDBT magnetic properties, that is, cross conjugated 4/8 should be affected less than linearly conjugated 3/7.

Although isolation of anti-IIDBT-S 7 proved elusive, we explored the diradical nature of syn-sulfone 8 first by variable temperature (VT) proton NMR spectroscopy. Based on its calculated $\Delta E_{\rm ST}$ (-8.29 kcal mol⁻¹), one would expect the need for slightly higher temperatures to populate the triplet state when compared to syn-IIDBT 4 ($-8.06 \text{ kcal mol}^{-1}$). Like its parent thiophene, sulfone 8 also displayed solubility issues at room temperature in either 1,1,2,2-tetrachloroethane-d2 (Figure S1) or 1,2-dichlorobenzene- d_4 (Figure S2). As was the case with 4, thermal broadening of the aromatic proton NMR signals of 8 (Figures 9a and S3) began at 75 °C, and resolution of the signals was almost lost by 125-130 °C. Interestingly, once the sample was cooled back to 25 °C, the solubility of 8 was greatly enhanced, and the signals could be completely assigned. Similar to the computations, these qualitative results suggest that compounds 4 and 8 have very similar singlet-triplet energy gaps.

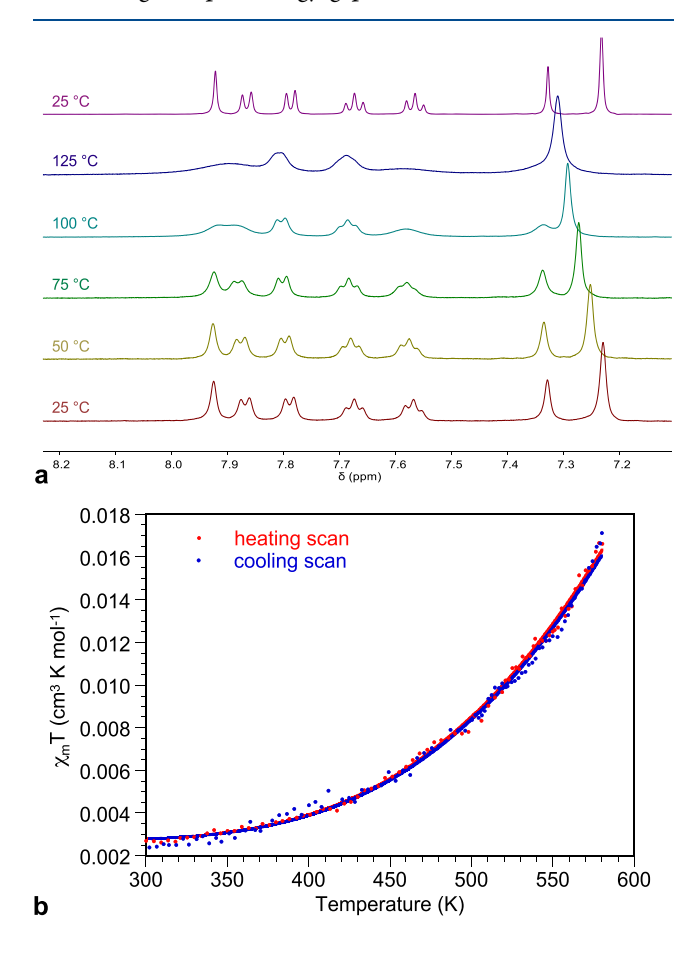


Figure 9. (a) VT 1 H NMR spectra of the aromatic region of **8** in 1,1,2,2-tetrachloroethane- d_2 . (b) SQUID magnetometry data for **8** in the solid state (circles) along with the corresponding Bleaney–Bowers fits of the heating and cooling curves (solid lines).

To experimentally examine the magnetic properties of the sole open-shell sulfone, superconducting quantum interference device (SQUID) magnetometry was performed on a sample of 8. The magnetic properties of 8 were measured up to \sim 580 K (Figure 9b), as the compound was shown by thermogravimetric analysis (TGA) to be stable at elevated temperatures (Figure S31). The SQUID signal was subjected to the Bleaney–Bowers fitting, 80 from which the singlet-triplet energy gap was calculated to be -6.5 kcal mol⁻¹, which is the average of two sets of heating and cooling experiments. With changes of <3% between the heating and cooling runs, these results are indicative of the thermal resilience of 8 at high temperatures. Although somewhat lower than the calculated $\Delta E_{\rm ST}$ (-8.29 kcal mol⁻¹), the experimental value, much like in the case of IIDBTs 3 and 4, supports the hypothesis of an open-shell molecule with a ground-state singlet and an accessible triplet state only at elevated temperatures.

CONCLUSIONS

A small family of benzothiophene-derived sulfones has been synthesized and fully characterized using a late-stage modification approach. Through the use of a single chemical transformation, we are able to alter the antiaromaticity in our IDBTs and the diradical character and related properties in syn-IIDBT. This work highlights the development of late-stage modification methods to impart meaningful change in properties without time-consuming alteration of the synthetic route. These resulting changes in antiaromaticity are trackable through proton NMR spectroscopy, NICS-XY scan calculations, and electrochemistry. The CV data show that while such modification increases the HOMO-LUMO energy gaps to a small degree, it lowers the HOMO and LUMO energy levels by 0.5-0.6 eV. The most significant change upon sulfone formation is flipping of the bond alternation pattern within the indacene core, as this relieves the potential destabilizing effects of enhanced paratropicity if the bond alternation where to retain a normal pattern. Notably, late-stage modification has provided an additional way to tune the diradical character and singlet-triplet energy gap of our ever-expanding series of diradicaloids, 58,60,62,63 garnering new hope for the implementation of diradicals into organic devices. Work is under way to develop additional late-stage modification approaches to finetune antiaromaticity and diradical character and related properties in our indeno[1,2-b]fluorene-derived scaffolds and to integrate some of these molecules into OFETs.

■ EXPERIMENTAL SECTION

General Procedures. All air-sensitive manipulations were carried out under an inert nitrogen gas using the standard Schlenk technique. For moisture-sensitive reactions, tetrahydrofuran (THF) and toluene were refluxed with Na benzophenone ketyl for 24 h prior to distillation and use. Silica gel (240-300 mesh) was used for column chromatography. All other reagents were purchased and used as received. NMR spectra were recorded using a Bruker AVANCE III HD 500 equipped with a Prodigy Multinuclear Cryoprobe (1H: 500 MHz) or Bruker AVANCE III HD 600 equipped with a Prodigy multinuclear cryoprobe (¹H: 600 MHz, ¹³C: 151 MHz) NMR spectrometer at room temperature (unless otherwise noted). ¹H and $^{1\bar{3}}$ C NMR chemical shifts (δ) are expressed in ppm relative to the residual nondeuterated solvent reference (CDCl₃: ¹H 7.26 ppm, ¹³C 77.16 ppm; CD₂Cl₂: ¹H 5.32 ppm, ¹³C 53.84 ppm; DMSO-*d*₆: ¹H 2.50 ppm, ^{13}C 39.52 ppm). UV-vis spectra were recorded using an Agilent Technologies Cary 60 UV-vis spectrometer in HPLC grade CHCl₃. 4-tert-Butyl-2,6-dimethylbromobenzene,⁸¹ diones 10–11,²⁷

diones 12-13,60,62 and 1-Mes^{27,67} were prepared according to the

General Procedure A: Preparation of Quinoidal Compounds 1-4. A flame-dried round bottom flask was charged with 4-tert-butyl-2,6-dimethylbromobenzene (6 equiv) dissolved in dry THF that was then cooled to -78 °C. Once the temperature was reached, n-BuLi (5.5 equiv) was added dropwise and the organolithiate was stirred at -78 °C for 1 h. Meanwhile, in a separate flamedried round bottom flask, a suspension of dione (1 equiv) in dry THF was also cooled to -78 °C to which the organolithiate was transferred via a cannula. The reaction was gradually warmed to room temperature overnight. The reaction was quenched with sat. NH₄Cl solution, and the organics were extracted with dichloromethane (DCM) (3x). The combined organic layer was then washed with H₂O and brine, dried (MgSO₄) and concentrated in vacuo. A short plug over SiO2 purified the resultant diols, which were carried on to the reductive dearomatization without further purification or characterization.

In a round-bottom flask, the crude diol (1 equiv) and anhydrous $SnCl_2$ (4 equiv) were dissolved in dry toluene. TFA (3 drops, catalytic) was added to the mixture which was then stirred for 4 h. The reaction was monitored via TLC (9:1 hexanes/DCM). Once the reaction was complete, the mixture was concentrated to ~ 10 mL and then poured over a silica plug, eluting with 1:1 hexanes/DCM to collect the crude reduced compounds. Column chromatography using an eluant of hexanes and DCM (see each compound for specific details) afforded the purified title compounds.

General Procedure B: Preparation of Sulfones. A flame-dried, foil-wrapped round-bottom flask equipped with a Claisen head was charged with compounds 1–4 (1 equiv) and dry DCM. To this, mCPBA (6 equiv) was added in three portions over a 30 min period. After stirring at room temperature for 21 h, the reaction was quenched with a 10% KOH solution, and the organics were extracted using DCM (3×). The combined organic layers were washed with brine, dried (MgSO₄), and then concentrated to dryness. Column chromatography using a mixture of hexanes and DCM as the eluant (see each compound for specific details) afforded the purified title compounds.

anti-IDBT 1. Following general procedure A, the lithiate generated from 4-tert-butyl-2,6-dimethylbromobenzene (0.92 g, 3.80 mmol) in THF (10 mL) and n-BuLi (2.2 mL, 3.49 mmol) was added to dione 10 (0.25 g, 0.63 mmol) in THF (20 mL) to produce the intermediate diol. A short SiO₂ plug using hexanes removed the nonpolar impurities, followed by 1:3 DCM/hexanes to collect the first diastereomer and pure DCM to collect the second diastereomer.

Following general procedure A, the diol mixture and SnCl₂ (0.30 g, 4 equiv) were reacted in rigorously degassed and dry toluene (40 mL). After the initial plug, column chromatography on SiO₂ using 15% DCM/hexanes gave 1 (138 mg, 32% from dione) as a deeppurple solid. $^1\mathrm{H}$ NMR (600 MHz, CDCl₃): δ 7.47 (d, J=7.9 Hz, 2H), 7.16 (s, 4H), 7.01 (t, J=6.9 Hz, 2H), 6.96 (t, J=7.5 Hz, 2H), 6.57 (dd, J=8.0, 1.3 Hz, 2H), 6.09 (s, 2H), 2.36 (s, 12H), 1.39 (s, 18H). $^{13}\mathrm{C}\{^1\mathrm{H}\}$ NMR (151 MHz, CDCl₃): δ 150.9, 148.1, 147.6, 143.7, 143.0, 136.7, 136.0, 133.0, 131.5, 129.8, 125.9, 125.4, 124.4, 123.8, 123.5, 120.6, 34.4, 31.4, 20.9. HRMS (TOF ES⁺) (m/z): calcd for $\mathrm{C_{48}H_{45}S_2}$ (M + H)⁺, 685.2963; found, 685.2939.

anti-IDBT-sulfone 5. Following general procedure B, 1 (90 mg, 0.13 mmol) was reacted with mCPBA (135 mg, 0.79 mmol) in dry DCM (15 mL). After the basic aqueous workup, the crude sulfone was purified by flash column chromatography using 45% DCM/ hexanes as the eluant to give 5 (41 mg, 54%) as a vibrant purple solid with a blue sheen. 1 H NMR (500 MHz, CDCl₃): δ 7.66 (d, J = 8.2 Hz, 2H), 7.38 (t, J = 8.0 Hz, 2H), 7.35 (td, J = 7.5, 1.2 Hz, 2H), 7.14 (s, 4H), 6.59 (d, J = 7.5 Hz, 2H), 6.03 (s, 2H), 2.34 (s, 12H), 1.38 (s, 18H). 13 C{ 1 H} NMR (126 MHz, CDCl₃): δ 152.2, 146.6, 146.4, 144.9, 142.3, 140.7, 135.7, 133.5, 130.73, 130.70, 129.3, 128.0, 126.9, 125.0, 122.0, 121.8, 34.5, 31.2, 20.8. HRMS (TOF ES⁺) (m/z): calcd for $C_{48}H_{45}O_4S_2$ (M + H)⁺, 749.2759; found, 749.2747.

anti-IDBT-sulfone 5-Mes. Following general procedure B, 1-Mes (81 mg, 0.13 mmol) was reacted with mCPBA (135 mg, 0.79 mmol)

syn-IDBT 2. Following general procedure A, the lithiate generated from 4-tert-butyl-2,6-dimethylbromobenzene (0.92 g, 3.80 mmol) in THF (10 mL) and n-BuLi (2.2 mL, 3.49 mmol) was added to dione 11 (0.25 g, 0.63 mmol) in THF (20 mL) to produce the intermediate diol. A short SiO₂ plug using hexanes removed nonpolar impurities, followed by 30% DCM/hexanes to collect the first diastereomer and pure DCM to collect the second diastereomer.

Following general procedure A, the diol mixture and $SnCl_2$ (0.39 g, 4 equiv) were reacted in rigorously degassed and dry toluene (45 mL). After the initial plug using 1:9 DCM/hexanes, preparatory TLC (1:3 DCM/hexanes) afforded 2 (164 mg, 38% from the dione) as a teal solid. Because of the low solubility of the title compound (peaks are of the same magnitude as that of the ¹³C satellite peaks), the residual solvent peaks are greatly exaggerated. ¹H NMR (600 MHz, CDCl₃): δ 7.45 (d, J = 8.1 Hz, 2H), 7.36 (d, J = 8.0 Hz, 2H), 7.14 (s, 4H), 7.11 (t, J = 7.2 Hz, 4H), 7.04 (t, J = 7.3 Hz, 2H), 6.06 (s, 2H), 2.45 (s, 12H), 1.39 (s, 18H). ¹³C{¹H} NMR (151 MHz, CDCl₃): δ 151.2, 148.1, 147.1, 146.6, 140.9, 137.5, 136.1, 134.9, 133.4, 129.4, 125.2, 124.7, 124.4, 124.3, 123.9, 121.8, 34.5, 31.4, 21.0. HRMS (TOF ASAP⁺) (m/z): calcd for $C_{48}H_{45}S_2$ (M + H)⁺, 685.2963; found, 685.2931.

syn-IDBT-sulfone 6. Following general procedure B, **2** (0.27 g, 0.40 mmol) was reacted with mCPBA (275 mg, 1.59 mmol) in dry DCM (40 mL). After the basic aqueous workup, the crude sulfone was purified by flash column chromatography using 2:1 DCM/hexanes as the eluant to give **6** (72 mg, 23%) as a bluish-violet solid. ¹H NMR (600 MHz, CDCl₃): δ 7.76 (dd, J = 7.2, 1.5 Hz, 2H), 7.62 (td, J = 6.6, 1.5 Hz, 2H), 7.60–7.55 (m, 4H), 7.17 (s, 4H), 6.91 (s, 2H), 2.40 (s, 12H), 1.38 (s, 18H). ¹³C{¹H} NMR (151 MHz, CDCl₃): δ 152.3, 147.9, 147.4, 146.8, 143.5, 138.7, 136.7, 133.7, 132.6, 131.6, 128.9, 126.8, 125.9, 125.6, 125.1, 122.9, 34.9, 31.7, 21.2. HRMS (TOF ES⁺) (m/z): calcd for C₄₈H₄₅O₄S₂ (M + H)⁺, 749.2759; found, 749.2749.

anti-IIDBT 3. Following general procedure A, the lithiate generated from 4-tert-butyl-2,6-dimethylbromobenzene (0.61 g, 2.52 mmol) in THF (20 mL) and n-BuLi (1.5 mL, 2.36 mmol) was added to dione 12 (0.14 g, 0.32 mmol) in THF (20 mL) to produce the intermediate diol. A short SiO₂ plug using hexanes removed nonpolar impurities, followed by 2:3 DCM/hexanes to collect the first diastereomer and pure DCM to collect the second diastereomer.

Following general procedure A, the diol mixture and $SnCl_2$ (0.20 g, 4 equiv) were reacted in rigorously degassed and dry toluene (40 mL). After the initial plug using 1:9 DCM/hexanes, the filtrate was concentrated. The solid was rinsed with cold MeCN (3×), and 3 was isolated as a deep-purple solid (97 mg, 42% from the dione). NMR spectra and mass spectrum matched the data previously reported.⁶²

Benzothiazine Dioxide 9. Compound 3 (0.18 g, 0.25 mmol, 1 equiv), UHP (0.24 g, 2.52 mmol, 10 equiv), and phthalic anhydride (0.37 g, 2.52 mmol, 10 equiv) were added to a flame-dried round-bottom flask equipped with a reflux condenser under an N_2 atmosphere. Dry EtOAc (25 mL) was added, and the reaction mixture was heated in a sand-filled heating mantle to 90 °C for 24 h. The reaction mixture was quenched with saturated Na_2SO_3 solution, and then, the organics were extracted with DCM (3×). The organics were washed sequentially with 1 M NaOH, H_2O , and brine, dried (MgSO₄), and concentrated in vacuo. Purification by preparatory TLC (DCM) and collecting the vibrant purple band with an R_f of 0.5. furnished 9 (22 mg, 11%) as a purplish-red solid. ¹H NMR (600 MHz, CDCl₃): δ 8.09 (s, 2H), 8.05 (d, J = 7.8 Hz, 2H), 7.48 (t, J =

7.5 Hz, 2H), 7.33–7.27 (m, 6H), 7.13 (s, 2H), 6.94 (d, J=8.2 Hz, 2H), 2.15 (s, 12H), 1.44 (s, 18H). $^{13}C\{^{1}H\}$ NMR (151 MHz, CDCl₃): δ 171.2, 157.9, 153.4, 142.4, 138.1, 134.6, 134.2, 133.2, 130.2, 128.5, 127.5, 126.4, 126.1, 125.1, 124.9, 120.9, 35.1, 31.7, 20.5. MS (TOF ES⁺) (m/z): calcd for $C_{52}H_{47}N_{2}O_{4}S_{2}$ (M + H)⁺, 827.2977; found, 827.2997.

syn-IIDBT 4. Following general procedure A, the lithiate generated from 4-tert-butyl-2,6-dimethylbromobenzene (0.82 g, 3.37 mmol) in THF (10 mL) and n-BuLi (1.9 mL, 3.09 mmol) was added to dione 13 (0.25 g, 0.56 mmol) in THF (20 mL) to produce the intermediate diol. A short SiO₂ plug using hexanes removed nonpolar impurities, followed by 45% DCM/hexanes to collect the first diastereomer and pure EtOAc to collect the second diastereomer.

Following general procedure A, the diol mixture and SnCl₂ (0.39 g, 4 equiv) were reacted in rigorously degassed and dry toluene (45 mL). After the initial plug using 1:9 DCM/hexanes, preparatory TLC of the crude material using 1:3 DCM/hexanes as the eluant gave 4 (149 mg, 36% from the dione) as a green solid. NMR spectra and mass spectrum matched those of the previously reported compound.⁶²

syn-IIDBT-sulfone 8. Following general procedure B, 4 (0.11 g, 0.15 mmol) was reacted with mCPBA (210 mg, 1.21 mmol) in dry DCM (20 mL). After the basic aqueous workup, the crude sulfone was purified by flash column chromatography using 2:1 DCM/hexanes as the eluant to give 8 (58 mg, 48%) as a greyish-purple solid. ¹H NMR (500 MHz, CDCl₃): δ 7.83 (s, 2H), 7.76–7.73 (m (overlapping dd), 4H), 7.58 (td, J = 7.7, 1.1 Hz, 2H), 7.48 (t, J = 7.4 Hz, 2H), 7.24 (s, 2H), 7.16 (s, 4H), 2.29 (s, 12H), 1.38 (s, 18H). ¹³C{¹H} NMR (151 MHz, CDCl₃): δ 152.1, 145.8, 142.3, 142.1, 141.4, 140.1, 136.9, 136.5, 135.4, 133.8, 131.1, 130.2, 130.0, 127.4, 127.1, 125.0, 124.0, 123.0, 34.9, 31.7, 21.0. HRMS (TOF ES⁺) (m/z): calcd for $C_{52}H_{46}O_4S_2$ (M)⁺, 798.2838; found, 798.2831.

ASSOCIATED CONTENT

Supporting Information

The Supporting Information is available free of charge at https://pubs.acs.org/doi/10.1021/acs.joc.0c01387.

¹H and ¹³C NMR spectra for all new compounds, additional UV-vis, X-ray, CV, and SQUID data, and computational details including the coordinates of optimized structures (PDF)

X-ray structure of 5-Mes (CIF)

X-ray structure of 6 (CIF)

X-ray structure of 8 (CIF)

X-ray structure of 9 (CIF)

AUTHOR INFORMATION

Corresponding Author

Michael M. Haley — Department of Chemistry & Biochemistry, The Materials Science Institute, and Phil and Penny Knight Campus for Accelerating Scientific Impact, University of Oregon, Eugene, Oregon 97403-1253, United States; orcid.org/0000-0002-7027-4141; Email: haley@uoregon.edu

Authors

Justin J. Dressler — Department of Chemistry & Biochemistry and The Materials Science Institute, University of Oregon, Eugene, Oregon 97403-1253, United States;

orcid.org/
0000-0002-0405-5653

Joshua E. Barker — Department of Chemistry & Biochemistry and The Materials Science Institute, University of Oregon, Eugene, Oregon 97403-1253, United States; orcid.org/0000-0001-6139-8858

- Lucas J. Karas Department of Chemistry, University of Houston, Houston, Texas 77204, United States; ⊚ orcid.org/ 0000-0001-7970-119X
- Hannah E. Hashimoto Department of Chemistry & Biochemistry and The Materials Science Institute, University of Oregon, Eugene, Oregon 97403-1253, United States
- Ryohei Kishi Department of Materials Engineering Science, Graduate School of Engineering Science, Osaka University, Toyonaka, Osaka 560-8531, Japan; orcid.org/0000-0002-6005-7629
- Lev N. Zakharov CAMCOR, University of Oregon, Eugene, Oregon 97403-1433, United States
- Samantha N. MacMillan Department of Chemistry & Chemical Biology, Cornell University, Ithaca, New York 14853, United States; Occid.org/0000-0001-6516-1823
- Carlos J. Gomez-Garcia Department of Inorganic Chemistry and Instituto de Ciencia Molecular, Universidad de Valencia, Paterna 46980, Spain; o orcid.org/0000-0002-0015-577X
- Masayoshi Nakano Department of Materials Engineering Science, Graduate School of Engineering Science, Center for Spintronics Research Network, Graduate School of Engineering Science, and Quantum Information and Quantum Biology Division, Institute for Open and Transdisciplinary Research Initiatives, Osaka University, Toyonaka, Osaka 560-8531, Japan; Oocid.org/0000-0002-3544-1290
- Judy I. Wu Department of Chemistry, University of Houston, Houston, Texas 77204, United States; ⊚ orcid.org/0000-0003-0590-5290

Complete contact information is available at: https://pubs.acs.org/10.1021/acs.joc.0c01387

Notes

The authors declare no competing financial interest.

ACKNOWLEDGMENTS

This work was supported by the US National Science Foundation (CHE-1565780 to MMH, CHE-1751370 to JIW), the National Institute of General Medical Sciences of the National Institute of Health (R35GM133528 to JIW), the Generalitat Valenciana (Prometeo2019/076), and by the Japan Society for the Promotion of Science (JSPS, KAKENHI Grants JP18H01943, JP17H05157, and JP26107004), the Kyoto Technoscience Center, and the Iketani Science and Technology Foundation. Mass spectrometry capabilities in the CAMCOR facility are supported by the NSF (CHE-1625529). We thank Dr. Casey Check for his assistance with acquiring and interpreting the TGA data. Theoretical calculations were partly performed using the Research Center for Computational Science, Okazaki, Japan.

REFERENCES

- (1) Giri, G.; Verploegen, E.; Mannsfeld, S. C. B.; Atahan-Evrenk, S.; Kim, D. H.; Lee, S. Y.; Becerril, H. A.; Aspuru-Guzik, A.; Toney, M. F.; Bao, Z. Tuning Charge Transport in Solution-Sheared Organic Semiconductors Using Lattice Strain. *Nature* **2011**, *480*, 504–508.
- (2) Payne, M. M.; Parkin, S. R.; Anthony, J. E. Functionalized Higher Acenes: Hexacene and Heptacene. *J. Am. Chem. Soc.* **2005**, 127, 8028–8029.
- (3) Fudickar, W.; Linker, T. Why Triple Bonds Protect Acenes from Oxidation and Decomposition. *J. Am. Chem. Soc.* **2012**, *134*, 15071–15082
- (4) Anthony, J. E. The Larger Acenes: Versatile Organic Semi-conductors. *Angew. Chem. Int.* **2008**, *47*, 452–483.

- (5) Zade, S. S.; Zamoshchik, N.; Reddy, A. R.; Fridman-Marueli, G.; Sheberla, D.; Bendikov, M. Products and Mechanism of Acene Dimerization. A Computational Study. *J. Am. Chem. Soc.* **2011**, *133*, 10803–10816.
- (6) Schleyer, P. v. R.; Manoharan, M.; Jiao, H.; Stahl, F. The Acenes: Is There a Relationship between Aromatic Stabilization and Reactivity? *Org. Lett.* **2001**, *3*, 3643–3646.
- (7) Chen, W.; Yu, F.; Xu, Q.; Zhou, G.; Zhang, Q. Recent Progress in High Linearly Fused Polycyclic Conjugated Hydrocarbons (PCHs, n > 6) with Well-Defined Structures. *Adv. Sci.* **2020**, *7*, 1903766.
- (8) Breslow, R.; Brown, J.; Gajewski, J. J. Antiaromaticity of Cyclopropenyl Anions. J. Am. Chem. Soc. 1967, 89, 4383–4390.
- (9) Breslow, R. Antiaromaticity. Acc. Chem. Res. 1973, 6, 393-398.
- (10) Krygowski, T. M.; Cyrañski, M. K.; Czarnocki, Z.; Häfelinger, G.; Katritzky, A. R. Aromaticity: A Theoretical Concept of Immense Practical Importance. *Tetrahedron* **2000**, *56*, 1783–1796.
- (11) Wiberg, K. B. Antiaromaticity in Monocyclic Conjugated Carbon Rings. Chem. Rev. 2001, 101, 1317–1332.
- (12) Chen, Z.; Wannere, C. S.; Corminboeuf, C.; Puchta, R.; Schleyer, P. v. R. Nucleus-Independent Chemical Shifts (NICS) as an Aromaticity Criterion. *Chem. Rev.* **2005**, *105*, 3842–3888.
- (13) Mills, N. S.; Llagostera, K. B. Summation of Nucleus Independent Chemical Shifts as a Measure of Aromaticity. *J. Org. Chem.* **2007**, 72, 9163–9169.
- (14) Kawase, T.; Fujiwara, T.; Kitamura, C.; Konishi, A.; Hirao, Y.; Matsumoto, K.; Kurata, H.; Kubo, T.; Shinamura, S.; Mori, H.; Miyazaki, E.; Takimiya, K. Dinaphthopentalenes: Pentalene Derivatives for Organic Thin-Film Transistors. *Angew. Chem., Int. Ed.* **2010**, 49, 7728–7732.
- (15) Dai, G.; Chang, J.; Shi, X.; Zhang, W.; Zheng, B.; Huang, K.-W.; Chi, C. Thienoacene-Fused Pentalenes: Syntheses, Structures, Physical Properties and Applications for Organic Field-Effect Transistors. *Chem.—Eur J.* **2015**, *21*, 2019–2028.
- (16) Oshima, H.; Fukazawa, A.; Yamaguchi, S. Facile Synthesis of Polycyclic Pentalenes with Enhanced Hückel Antiaromaticity. *Angew. Chem., Int. Ed.* **2017**, *56*, 3270–3274.
- (17) Konishi, A.; Okada, Y.; Nakano, M.; Sugisaki, K.; Sato, K.; Takui, T.; Yasuda, M. Synthesis and Characterization of Dibenzo-[a_tf]pentalene: Harmonization of the Antiaromatic and Singlet Biradical Character. J. Am. Chem. Soc. **2017**, 139, 15248–15287.
- (18) Konishi, A.; Okada, Y.; Kishi, R.; Nakano, M.; Yasuda, M. Enhancement of Antiaromatic Character via Additional Benzoannulation in Dibenzo[a_f]pentalene: Synthesis and Properties of Benzo-[a]naphtho[2,1-f]pentalene and Dinaphtho[2,1-a_f]pentalene. J. Am. Chem. Soc. 2019, 141, 560–571.
- (19) Kato, S.-i.; Kuwako, S.; Takahashi, N.; Kijima, T.; Nakamura, Y. Benzo-and Naphthopentalenes: Syntheses, Structures, and Properties. *J. Org. Chem.* **2016**, *81*, 7700–7710.
- (20) Yuan, B.; Zhuang, J.; Kirmess, K. M.; Bridgmohan, C. N.; Whalley, A. C.; Wang, L.; Plunkett, K. N. Pentaleno[1,2-a:4,5']-diacenaphthylenes: Uniquely Stabilized Pentalene Derivatives. *J. Org. Chem.* **2016**, *81*, 8312–8318.
- (21) Cao, J.; London, G.; Dumele, O.; von Wantoch Rekowski, M.; Trapp, N.; Ruhlmann, L.; Boudon, C.; Stanger, A.; Diederich, F. The Impact of Antiaromatic Subunits in [4n+2] π -Systems: Bispentalenes with [4n+2] π -Electron Perimeters and Antiaromatic Character. *J. Am. Chem. Soc.* 2015, 137, 7178–7188.
- (22) Dai, G.; Chang, J.; Zhang, W.; Bai, S.; Huang, K.-W.; Xu, J.; Chi, C. Dianthraceno[a,e]pentalenes: Synthesis, Crystallographic Structures and Applications in Organic Field-Effect Transistors. *Chem. Commun.* **2015**, *51*, 503–506.
- (23) Wang, J.; Chu, M.; Fan, J.-X.; Lau, T.-K.; Ren, A.-M.; Lu, X.; Miao, Q. Crystal Engineering of Biphenylene-Containing Acenes for High-Mobility Organic Semiconductors. *J. Am. Chem. Soc.* **2019**, *141*, 3589–3596.
- (24) Jin, Z.; Teo, Y. C.; Teat, S. J.; Xia, Y. Regioselective Synthesis of [3] Naphthylenes and Tuning of Their Antiaromaticity. *J. Am. Chem. Soc.* **2017**, *139*, 15933–15939.

- (25) Jin, Z.; Yao, Z.-F.; Barker, K. P.; Pei, J.; Xia, Y. Dinaphthobenzo[1,2:4,5]dicyclobutadiene: Antiaromatic and Orthogonally Tunable Electronics and Packing. *Angew. Chem., Int. Ed.* **2019**, 58, 2034–2039.
- (26) Teo, Y. C.; Jin, Z.; Xia, Y. Synthesis of Cyclobutadienoid-Fused Phenazines with Strongly Modulated Degrees of Antiaromaticity. *Org. Lett.* **2018**, *20*, 3300–3304.
- (27) Marshall, J. L.; Uchida, K.; Frederickson, C. K.; Schütt, C.; Zeidell, A. M.; Goetz, K. P.; Finn, T. W.; Jarolimek, K.; Zakharov, L. N.; Risko, C.; Herges, R.; Jurchescu, O. D.; Haley, M. M. Indacenodibenzothiophenes: Synthesis, Optoelectronic Properties and Materials Applications of Molecules with Strong Antiaromatic Character. *Chem. Sci.* 2016, 7, 5547–5558.
- (28) Frederickson, C. K.; Zakharov, L. N.; Haley, M. M. Modulating Paratropicity Strength in Diareno-Fused Antiaromatics. *J. Am. Chem. Soc.* **2016**, *138*, 16827–16838.
- (29) Frederickson, C. K.; Rose, B. D.; Haley, M. M. Explorations of the Indenofluorenes and Expanded Quinoidal Analogues. *Acc. Chem. Res.* **2017**, *50*, 977–987.
- (30) Melidonie, J.; Liu, J.; Fu, Y.; Weigand, J. J.; Berger, R.; Feng, X. Pyrene-Fused s-Indacene. *J. Org. Chem.* **2018**, *83*, 6633–6639.
- (31) Broløs, L.; Kilde, M. D.; Hammerich, O.; Nielsen, M. B. Toward Redox-Active Indenofluorene-Extended Tetrathiafulvalene Oligomers—Synthesis and Studies of Dimeric Scaffolds. *J. Org. Chem.* **2020**, *85*, 3277—3286.
- (32) Ie, Y.; Sato, C.; Yamamoto, K.; Nitani, M.; Aso, Y. A Thiazole-Fused Antiaromatic Compound Containing an s-Indacene Chromophore with a High Electron Affinity. *Chem. Lett.* **2018**, 47, 1534–1537.
- (33) Jiang, Q.; Tao, T.; Phan, H.; Han, Y.; Gopalakrishna, T. Y.; Herng, T. S.; Li, G.; Yuan, L.; Ding, J.; Chi, C. Diazuleno-s-Indacene Diradicaloids: Syntheses, Properties, and Local (Anti)Aromaticity Shift from Neutral to Dicationic State. *Angew. Chem., Int. Ed.* **2018**, *57*, 16737–16741.
- (34) Breslow, R.; Schneebeli, S. T. Structure-Property Relationships in Molecular Wires. *Tetrahedron* **2011**, *67*, 10171–10178.
- (35) Breslow, R.; Foss, F. W., Jr. Charge Transport in Nanoscale Aromatic and Antiaromatic Systems. *J. Phys. Condens. Matter* **2008**, 20, 374104.
- (36) Chen, W.; Li, H.; Widawsky, J. R.; Appayee, C.; Venkataraman, L.; Breslow, R. Aromaticity Decreases Single-Molecule Junction Conductance. *J. Am. Chem. Soc.* **2014**, *136*, 918–920.
- (37) Mahendran, A.; Gopinath, P.; Breslow, R. Single Molecule Conductance of Aromatic, Nonaromatic, and Partially Antiaromatic Systems. *Tetrahedron Lett.* **2015**, *56*, 4833–4835.
- (38) Zeidell, A. M.; Jennings, L.; Frederickson, C. K.; Ai, Q.; Dressler, J. J.; Zakharov, L. N.; Risko, C.; Haley, M. M.; Jurchescu, O. D. Organic Semiconductors Derived from Dinaphtho-Fused s-Indacenes: How Molecular Structure and Film Morphology Influence Thin-Film Transistor Performance. *Chem. Mater.* **2019**, *31*, 6962–6970.
- (39) Liu, C.; Xu, S.; Zhu, W.; Zhu, X.; Hu, W.; Li, Z.; Wang, Z. Diaceno[*a,e*]pentalenes: An Excellent Molecular Platform for High-Performance Organic Semiconductors. *Chem.—Eur J.* **2015**, *21*, 17016–17022.
- (40) Gopalakrishna, T. Y.; Zeng, W.; Lu, X.; Wu, J. From Open-Shell Singlet Diradicaloids to Polyradicaloids. *Chem. Commun.* **2018**, 54, 2186–2199.
- (41) Koike, H.; Chikamatsu, M.; Azumi, R.; Tsutsumi, J.; Ogawa, K.; Yamane, W.; Nishiuchi, T.; Kubo, T.; Hasegawa, T.; Kanai, K. Stable Delocalized Singlet Biradical Hydrocarbon for Organic Field-Effect Transistors. *Adv. Funct. Mater.* **2016**, *26*, 277–283.
- (42) Morita, Y.; Suzuki, S.; Sato, K.; Takui, T. Synthetic Organic Spin Chemistry for Structurally Well-Defined Open-Shell Graphene Fragments. *Nat. Chem.* **2011**, *3*, 197–204.
- (43) Morita, Y.; Nishida, S.; Murata, T.; Moriguchi, M.; Ueda, A.; Satoh, M.; Arifuku, K.; Sato, K.; Takui, T. Organic Tailored Batteries Materials Using Stable Open-Shell Molecules with Degenerate Frontier Orbitals. *Nat. Mater.* **2011**, *10*, 947–951.

- (44) Smith, M. B.; Michl, J. Recent Advances in Singlet Fission. *Annu. Rev. Phys. Chem.* **2013**, *64*, 361–386.
- (45) Minami, T.; Nakano, M. Diradical Character View of Singlet Fission. *J. Phys. Chem. Lett.* **2012**, *3*, 145–150.
- (46) Juríček, M.; Ravat, P.; Šolomek, T.; Ribar, P. Biradicaloid with a Twist: Lowering the Singlet-Triplet Gap. *Synlett* **2016**, *27*, 1613–1617.
- (47) Di Motta, S.; Negri, F.; Fazzi, D.; Castiglioni, C.; Canesi, E. V. Biradicaloid and Polyenic Character of Quinoidal Oligothiophenes Revealed by the Presence of a Low-Lying Double-Exciton State. *J. Phys. Chem. Lett.* **2010**, *1*, 3334–3339.
- (48) Abe, M. Diradicals. Chem. Rev. 2013, 113, 7011-7088.
- (49) Kubo, T.; Shimizu, A.; Sakamoto, M.; Uruichi, M.; Yakushi, K.; Nakano, M.; Shiomi, D.; Sato, K.; Takui, T.; Morita, Y.; Nakasuji, K. Synthesis, Intermolecular Interaction, and Semiconductive Behavior of a Delocalized Singlet Biradical Hydrocarbon. *Angew. Chem., Int. Ed.* **2005**, *44*, 6564–6568.
- (50) Shimizu, A.; Kubo, T.; Uruichi, M.; Yakushi, K.; Nakano, M.; Shiomi, D.; Sato, K.; Takui, T.; Hirao, Y.; Matsumoto, K.; Kurata, H.; Morita, Y.; Nakasuji, K. Alternating Covalent Bonding Interactions in a One-Dimensional Chain of a Phenalenyl-Based Singlet Biradical Molecule Having Kekulé Structures. *J. Am. Chem. Soc.* **2010**, *132*, 14421–14428.
- (51) Shimizu, A.; Hirao, Y.; Matsumoto, K.; Kurata, H.; Kubo, T.; Uruichi, M.; Yakushi, K. Aromaticity and π -Bond Covalency: Prominent Intermolecular Covalent Bonding Interaction of a Kekulé Hydrocarbon with Very Significant Singlet Biradical Character. *Chem. Commun.* **2012**, *48*, 5629–5631.
- (52) Hu, P.; Wu, J. Modern Zethrene Chemistry. Can. J. Chem. 2017, 95, 223-233.
- (53) Zeng, W.; Sun, Z.; Herng, T. S.; Gonçalves, T. P.; Gopalakrishna, T. Y.; Huang, K.-W.; Ding, J.; Wu, J. Super-Heptazethrene. *Angew. Chem., Int. Ed.* **2016**, *55*, 8615–8619.
- (54) Sun, Z.; Lee, S.; Park, K. H.; Zhu, X.; Zhang, W.; Zheng, B.; Hu, P.; Zeng, Z.; Das, S.; Li, Y.; Chi, C.; Li, R.-W.; Huang, K.-W.; Ding, J.; Kim, D.; Wu, J. Dibenzoheptazethrene Isomers with Different Biradical Characters: An Exercise of Clar's Aromatic Sextet Rule in Singlet Biradicaloids. *J. Am. Chem. Soc.* **2013**, *135*, 18229–18236.
- (55) Li, Y.; Heng, W.-K.; Lee, B. S.; Aratani, N.; Zafra, J. L.; Bao, N.; Lee, R.; Sung, Y. M.; Sun, Z.; Huang, K.-W.; Webster, R. D.; López Navarrete, J. T.; Kim, D.; Osuka, A.; Casado, J.; Ding, J.; Wu, J. Kinetically Blocked Stable Heptazethrene and Octazethrene: Closed-Shell or Open-Shell in the Ground State? *J. Am. Chem. Soc.* **2012**, *134*, 14913–14922.
- (56) Shimizu, A.; Kishi, R.; Nakano, M.; Shiomi, D.; Sato, K.; Takui, T.; Hisaki, I.; Miyata, M.; Tobe, Y. Indeno[2,1-b]fluorene: A 20-π-Electron Hydrocarbon with Very Low-Energy Light Absorption. *Angew. Chem., Int. Ed.* **2013**, *52*, 6076–6079.
- (57) Dressler, J. J.; Zhou, Z.; Marshall, J. L.; Kishi, R.; Takamuku, S.; Wei, Z.; Spisak, S. N.; Nakano, M.; Petrukhina, M. A.; Haley, M. M. Synthesis of the Unknown Indeno[1,2-a]fluorene Regioisomer: Crystallographic Characterization of Its Dianion. *Angew. Chem., Int. Ed.* **2017**, *56*, 15363–15367.
- (58) Rudebusch, G. E.; Zafra, J. L.; Jorner, K.; Fukuda, K.; Marshall, J. L.; Arrechea-Marcos, I.; Espejo, G. L.; Ponce Ortiz, R.; Gómez-García, C. J.; Zakharov, L. N.; Nakano, M.; Ottosson, H.; Casado, J.; Haley, M. M. Diindeno-Fusion of an Anthracene as a Design Strategy for Stable Organic Biradicals. *Nat. Chem.* **2016**, *8*, 753–759.
- (59) Miyoshi, H.; Miki, M.; Hirano, S.; Shimizu, A.; Kishi, R.; Fukuda, K.; Shiomi, D.; Sato, K.; Takui, T.; Hisaki, I.; Nakano, M.; Tobe, Y. Fluoreno[2,3-b]fluorene vs Indeno[2,1-b]fluorene: Unusual Relationship between the Number of π Electrons and Excitation Energy in m-Quinodimethane-Type Singlet Diradicaloids. J. Org. Chem. 2017, 82, 1380–1388.
- (60) Dressler, J. J.; Teraoka, M.; Espejo, G. L.; Kishi, R.; Takamuku, S.; Gómez-García, C. J.; Zakharov, L. N.; Nakano, M.; Casado, J.; Haley, M. M. Thiophene and Its Sulfur Inhibit Indenoindenodiben-

- zothiophene Diradicals from Low-Energy Lying Thermal Triplets. *Nat. Chem.* **2018**, *10*, 1134–1140.
- (61) Hacker, A. S.; Pavano, M.; Wood, J. E.; Hashimoto, H.; D'Ambrosio, K. M.; Frederickson, C. K.; Zafra, J. L.; Gómez-García, C. J.; Postils, V.; McDonald, A. R.; Casanova, D.; Frantz, D. K.; Casado, J. Fluoreno[2,1-a]fluorene: an ortho-naphthoquinodimethane-based system with partial diradical character. *Chem. Commun.* **2019**, *55*, 14186–14189.
- (62) Barker, J. E.; Dressler, J. J.; Cárdenas Valdivia, A.; Kishi, R.; Strand, E. T.; Zakharov, L. N.; MacMillan, S. N.; Gómez-García, C. J.; Nakano, M.; Casado, J.; Haley, M. M. Molecule Isomerism Modulates the Diradical Properties of Stable Singlet Diradicaloids. *J. Am. Chem. Soc.* 2020, 142, 1548–1555.
- (63) Dressler, J. J.; Cárdenas Valdivia, A.; Kishi, R.; Rudebusch, G. E.; Ventura, A. M.; Chastain, B. E.; Gómez-García, C. J.; Zakharov, L. N.; Nakano, M.; Casado, J.; Haley, M. M. Diindenoanthracene Diradicaloids Enable Rational, Incremental Tuning of Their Singlet-Triplet Energy Gaps. *Chem* **2020**, *6*, 1353–1368.
- (64) Majewski, M. A.; Chmielewski, P. J.; Chien, A.; Hong, Y.; Lis, T.; Witwicki, M.; Kim, D.; Zimmerman, P. M.; Stępień, M. 5,10-Dimesityldiindeno [1,2-a:2',1'-i]phenanthrene: A Stable Biradicaloid Derived from Chichibabin's Hydrocarbon. *Chem. Sci.* **2019**, *10*, 3413–3420.
- (65) Lu, R.-Q.; Wu, S.; Yang, L.-L.; Gao, W.-B.; Qu, H.; Wang, X.-Y.; Chen, J.-B.; Tang, C.; Shi, H.-Y.; Cao, X.-Y. Stable Diindeno-Fused Corannulene Regioisomers with Open-Shell Singlet Ground States and Large Diradical Characters. *Angew. Chem., Int. Ed.* **2019**, 58, 7600–7605.
- (66) Zeng, Z.; Shi, X.; Chi, C.; López Navarrete, J. T.; Casado, J.; Wu, J. Pro-Aromatic and Anti-Aromatic π-Conjugated Molecules: An Irresistible Wish to Be Diradicals. *Chem. Soc. Rev.* **2015**, *44*, 6578–6596.
- (67) Young, B. S.; Chase, D. T.; Marshall, J. L.; Vonnegut, C. L.; Zakharov, L. N.; Haley, M. M. Synthesis and Properties of Fully-Conjugated Indacenedithiophenes. *Chem. Sci.* **2014**, *5*, 1008–1014.
- (68) Yoshida, T.; Takahashi, K.; Ide, Y.; Kishi, R.; Fujiyoshi, J.-y.; Lee, S.; Hiraoka, Y.; Kim, D.; Nakano, M.; Ikeue, T.; Yamada, H.; Shinokubo, H. Benzonorcorrole NiII Complexes: Enhancement of Paratropic Ring Current and Singlet Diradical Character by Benzo-Fusion. *Angew. Chem., Int. Ed.* 2018, *57*, 2209–2213.
- (69) Wei, S.; Xia, J.; Dell, E. J.; Jiang, Y.; Song, R.; Lee, H.; Rodenbough, P.; Briseno, A. L.; Campos, L. M. Bandgap Engineering through Controlled Oxidation of Polythiophenes. *Angew. Chem., Int. Ed.* **2014**, *53*, 1832–1836.
- (70) Pappenfus, T. M.; Seidenkranz, D. T.; Lovander, M. D.; Beck, T. L.; Karels, B. J.; Ogawa, K.; Janzen, D. E. Synthesis and Electronic Properties of Oxidized Benzo[1,2-b:4,5-b']dithiophenes. *J. Org. Chem.* **2014**, *79*, 9408–9412.
- (71) Liu, G.; Zhang, H.; Huang, Y.; Han, Z.; Liu, G.; Liu, Y.; Dong, X.-Q.; Zhang, X. Efficient Synthesis of Chiral 2,3-Dihydrobenzo[b]-thiophene 1,1-Dioxides via Rh-Catalyzed Hydrogenation. *Chem. Sci.* 2019, 10, 2507–2512.
- (72) Barbarella, G.; Pudova, O.; Arbizzani, C.; Mastragostino, M.; Bongini, A. Oligothiophene-S.,S-Dioxides: A New Class of Thiophene-Based Materials. *J. Am. Chem. Soc.* **1998**, *63*, 1742–1745.
- (73) Dell, E. J.; Campos, L. M. The Preparation of Thiophene-S,S-Dioxides and Their Role in Organic Electronics. *J. Mater. Chem.* **2012**, 22, 12945–12952.
- (74) Gershoni-Poranne, R.; Stanger, A. The NICS-XY-Scan: Identification of Local and Global Ring Currents in Multi-Ring Systems. *Chem.—Eur J.* **2014**, *20*, 5673–5688.
- (75) Stanger, A. Nucleus-Independent Chemical Shifts (NICS): Distance Dependence and Revised Criteria for Aromaticity and Antiaromaticity. *J. Org. Chem.* **2006**, *71*, 883–893.
- (76) Even though NBO recognizes the resonance forms we draw for the dianion reference molecules, NRT analyses (which would give us the relative weights for a few of the most important resonance forms) would not finish because of a very large number (1000+) of potential resonance forms.

- (77) Gimarc, B. M. Topological Charge Stabilization. *J. Am. Chem. Soc.* 1983, 105, 1979–1984.
- (78) Despite multiple efforts, we were unable to obtain a suitable structure for 5 with the *t*-Mes groups. Regardless, our prior studies have shown that use of different bulky aryl groups attached to the apical carbons has minimal effect on the molecular geometry of the π -expanded conjugated system; see refs 60 and 62.
- (79) It is worth noting that no bond-flipped minima structures were found for 1 or 2 as both prefer a "normal" bonding pattern.
- (80) Bleaney, B.; Bowers, K. D. Anomalous Paramagnetism of Copper Acetate. *Proc. Roy. Soc. Lond. Math. Phys. Sci.* **1952**, 214, 451–465.
- (81) Field, J. E.; Hill, T. J.; Venkataraman, D. Bridged Triarylamines: A New Class of Heterohelicenes. *J. Org. Chem.* **2003**, *68*, 6071–6078.